Recording earthquakes for tomographic imaging of the mantle beneath the South Pacific by autonomous MERMAID floats

Joel D. Simon, Frederik J. Simons & Jessica C.E. Irving

Princeton University | University of Bristol

Every 6.25 days on average, data are returned from a mobile array of freely floating diving instruments, named MERMAID for Mobile Earthquake Recording in Marine Areas by Independent Divers, launched in French Polynesia in late 2018. Overall 50 MERMAIDs were deployed over a number of cruises (GEOAZUR, GENAVIR, IFREMER, JAMSTEC, SUSTECH) in this vast and understudied oceanic province as part of the collaborative South Pacific Plume Imaging and Modeling (SPPIM) project, under the aegis of the international EarthScope-Oceans consortium founded in 2016. Our objective is the hydroacoustic recording, from within the oceanic water column, of the seismic wavefield generated by earthquakes worldwide, and the nearly real-time transmission by satellite of these data, collected above and in the periphery of the South Pacific Superswell. This region, characterized by anomalously elevated oceanic crust and myriad seamounts, is believed to be the surface expression of deeply rooted mantle upwellings. Tomographically imaging Earth's mantle under the South Pacific with data from these novel instruments requires a careful examination of the earthquake-to-MERMAID travel times of the high-frequency P-wave detections within the windows selected for reporting by the discrimination algorithms on board. Our workflow picks the relevant arrivals, matches them to known earthquakes in global (e.g., CMT) earthquake catalogs, calculates their travel-time residuals with respect to global seismic reference models, characterizes their quality, and estimates their uncertainty. The lifespan of an individual MERMAID is five years. The utility for seismic tomography of MERMAID data quality is demonstrated by comparison against "traditional" land seismometers and Raspberry Shake sensors, using waveforms recovered from instrumented island stations in the geographic neighborhood of our floats. Our growing database of automatically accumulating 200–250 s long triggered segments contains a treasure trove for geophysicists—also for those interested in seismology beyond P-wave tomography. Equipped with two-way communication capabilities, MERMAID can furthermore entertain requests to deliver data from its one-year buffer, e.g., to study later-arriving seismic phases and also T-waves.

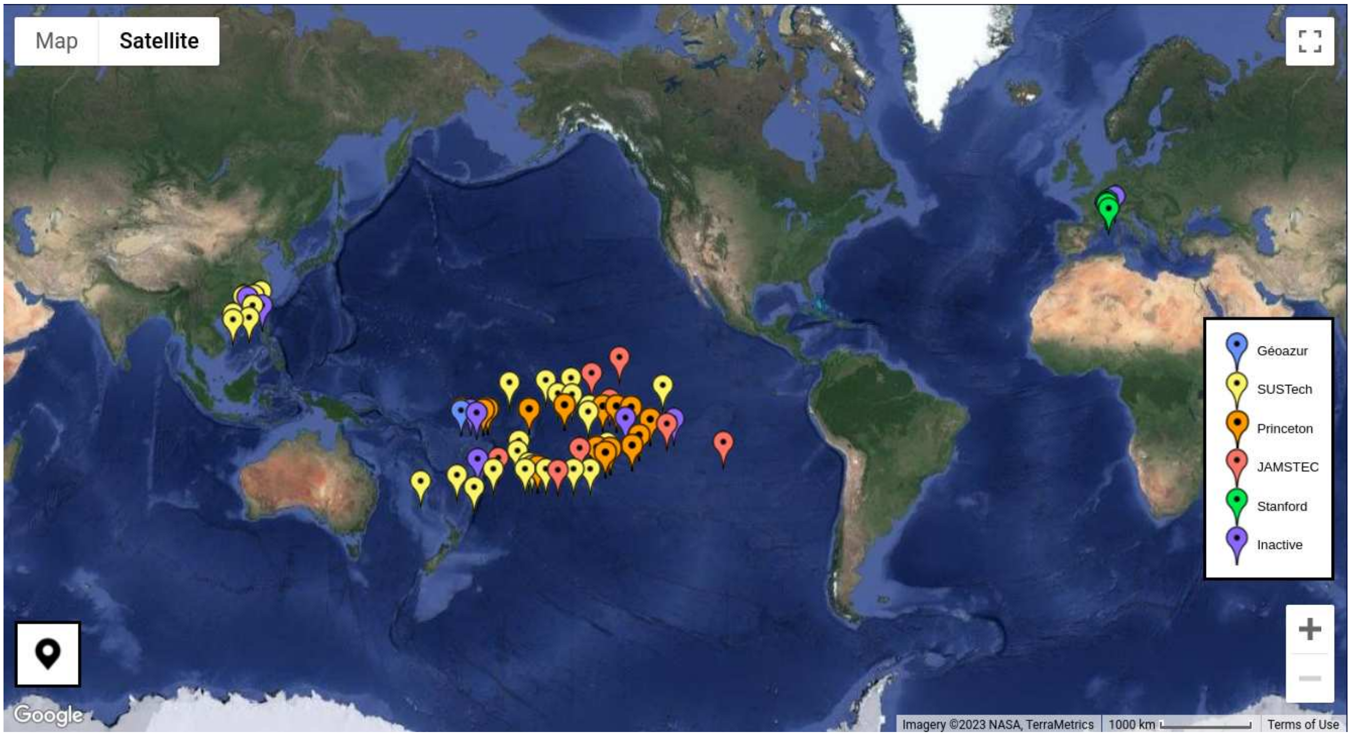

Figure 1: *Current global* MERMAID *fleet, as of 10 March 2023.* `http://www.earthscopeoceans.org`

Seismic evidence for a 1000 km mantle discontinuity under the Pacific

Zhendong Zhang, Jessica C.E. Irving,
Frederik J. Simons & Tariq Alkhalifah

Princeton University | MIT | University of Bristol | KAUST

Seismic discontinuities in the mantle are indicators of its thermo-chemical state and offer clues to its dynamics. Ray-based seismic methods, though limited by the approximations made, have mapped mantle transition zone discontinuities in detail, but have yet to offer definitive conclusions on the presence and nature of mid-mantle discontinuities. We developed a wave-equation-based imaging method, reverse-time migration of precursors to surface-reflected seismic body waves, to uncover both mantle transition zone and mid-mantle discontinuities, and interpret their physical nature. Using USArray data, we observe a thinned mantle transition zone southeast of Hawaii, and a reduction in impedance contrast around 410 km depth in the same area, suggesting a hotter-than-average mantle in the region. We furthermore reveal a 4000–5000 km-wide reflector in new images of the mid mantle below the central Pacific, at 950–1050 km depth. This deep discontinuity exhibits strong topography and generates reflections with polarity opposite to those originating at the 660 km discontinuity, implying an impedance reversal near 1000 km. We link this mid-mantle discontinuity to the upper reaches of deflected mantle plumes upwelling in the region. Reverse-time migration full-waveform imaging is a powerful approach to imaging Earth's interior, capable of broadening our understanding of its structure and dynamics and shrinking modeling uncertainties.

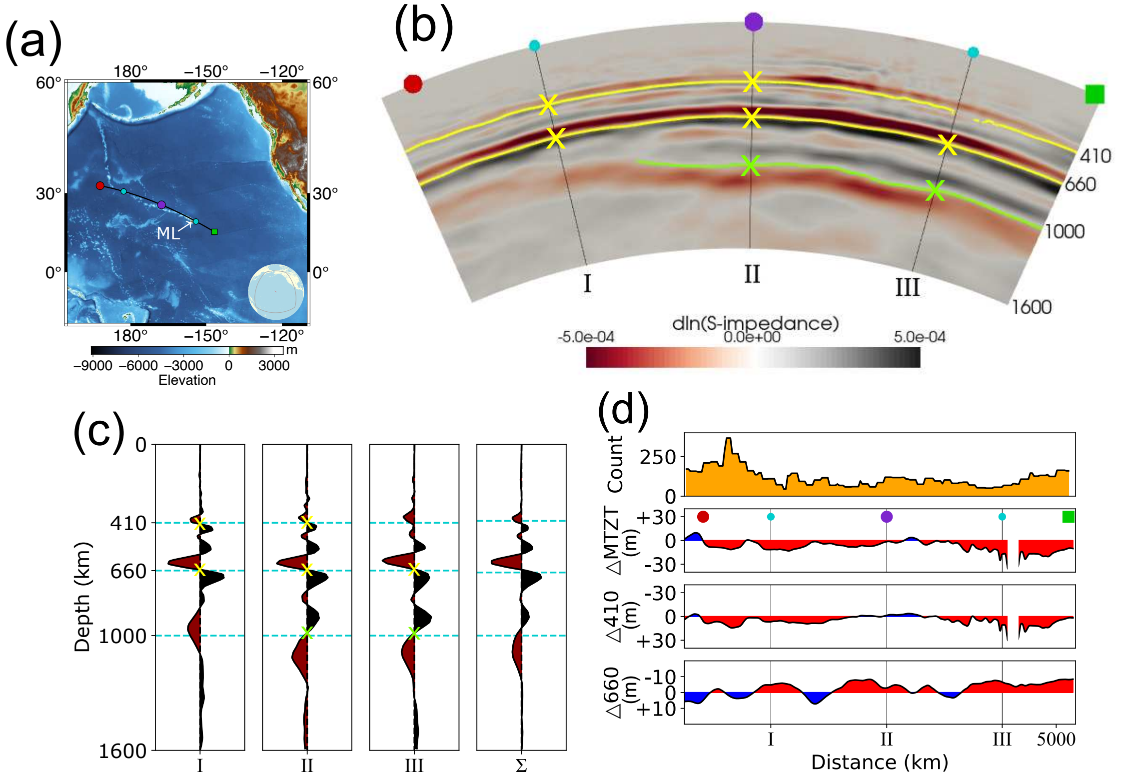

Figure 1: *Reverse-time migration image of mantle transition zone and mid-mantle discontinuities along the Hawaiian seamount chain. (a) Geographical situation. (b) Vertical slice through the imaged impedance contrasts. Traced 410, 660 and 100 km discontinuities are drawn in yellow. Three vertical profiles through this section are plotted in (c). Their stacked profile is in the last panel. (d) Topography of the mantle transition zone discontinuities. The first row shows bounce point counts along the Hawaiian seamount chain.* `http://doi.org/10.1038/s41467-023-37067-x`

A new horizon for deep ocean seafloor geodesy

Harold T. "Bud" Vincent & Frederik J. Simons

DBV Technology | Princeton University

In 2023 we conducted a first-of-its-kind technology demonstration in seafloor geodesy, in the deepest part of the Atlantic Ocean where it meets the Caribbean Sea, a complex geologic area known as the Puerto Rico Trench. Specifically, the demonstration consisted of deploying a solar-powered SeaTrac SP-48 uncrewed surface vehicle (USV) equipped with a DBV Technology GNSS-Acoustic Surface System to execute survey transects in open ocean while communicating with novel Deep Ocean Geodetic sensors (DOGs) submerged in the trench at depths of up to 5,500 m. The USV operated autonomously while being monitored and controlled from shore by satellite at two remote locations. The DOGs and SP-48 were deployed from RV Blue Manta. SeaTrac demonstrated excellent seakeeping ability (+/- 3 m cross track error) over sustained survey legs exceeding 20 km. Additionally, the platform demonstrated the ability to provide enough power to operate the surface acoustic system with limited self noise. Acoustic testing consisted of bi-directional transmissions from shore, to the sea surface via satellite, down to the seafloor and back again at horizontal distances up to 11 km. Transmissions included signals for synchronization, survey, command and control, and data telemetry. The DOGs contain a Chip Scale Atomic Clock for precise synchronization with GPS to enable sub-centimeter level positioning of the sensors on the seafloor. DOGs use very low power, and are suitable for very long-term deployments, more accurately and economically than possible using present methods. T-DOGs are recoverable and intended for deployments up to 3 years. C-DOGs are designed to last 30-50 years and are not intended to be recovered.

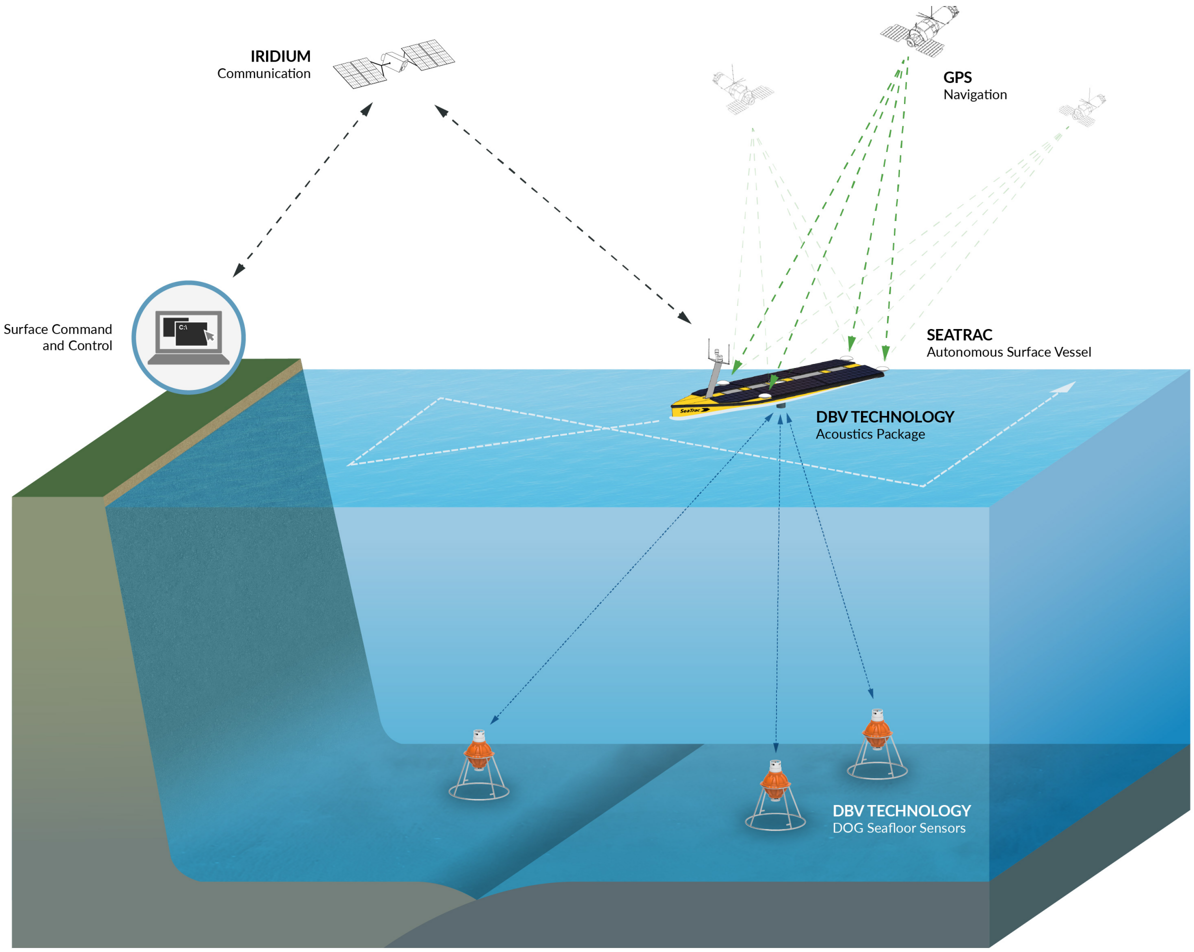

Figure 1: *Schematic of the successful test of the DBV/Princeton/SeaTrac system for deep ocean geodetic surveying in the Puerto Rican trench.* *Graphic by Mike Dunne,* `https://mikedunne.net`

On the origin of secondary microseism Love waves

Lucia Gualtieri, Etienne Bachmann, Frederik J. Simons & Jeroen Tromp

Princeton University | Stanford University

The interaction of ocean surface waves produces pressure fluctuations at the seafloor capable of generating seismic waves in the solid Earth. Secondary microseisms are the strongest terrestrial background seismic vibrations and account for the majority of the global seismographic data volume. They are generated by wind-driven ocean storms, whose energy couples with the solid Earth at the seafloor. Traditional generation theories for secondary microseisms satisfactorily explained secondary microseisms of the Rayleigh type but the accepted mechanism was unable to justify the presence of horizontally (transversely) polarized *Love* surface waves, which nevertheless have been observed in seismic data since the beginning of the twentieth century. Hence, an explanation for two-thirds of the worldwide ambient wavefield was wanting for over a century. Using unprecedented high-frequency numerical simulations of global seismic wave propagation, we have shed light on this hundred-year-old conundrum. These challenging numerical simulations help explain the origin of secondary microseism Love waves as being generated for a small fraction by boundary force-splitting at bathymetric inclines—but the majority is generated by the interaction of the seismic wavefield with wavespeed heterogeneity within the Earth. Secondary microseismic Love waves originate ergodically due to lateral heterogeneities in Earth structure. Our modeling quantitatively explains the observed seismic wave partitioning, accounts both for the effect of three-dimensional heterogeneity and for bathymetric force splitting, which is of minor importance but strongest in the steepest portions of midocean ridges and near ocean-continent boundaries. Small and well-focused Love-wave arrivals are observed at some seismographic stations, at great distances from storm sources, with strong seasonality observed in the shortest period bands (below 7 s). Our understanding of these processes is important to account for realistic source distributions in full-wavefield ambient-noise tomography.

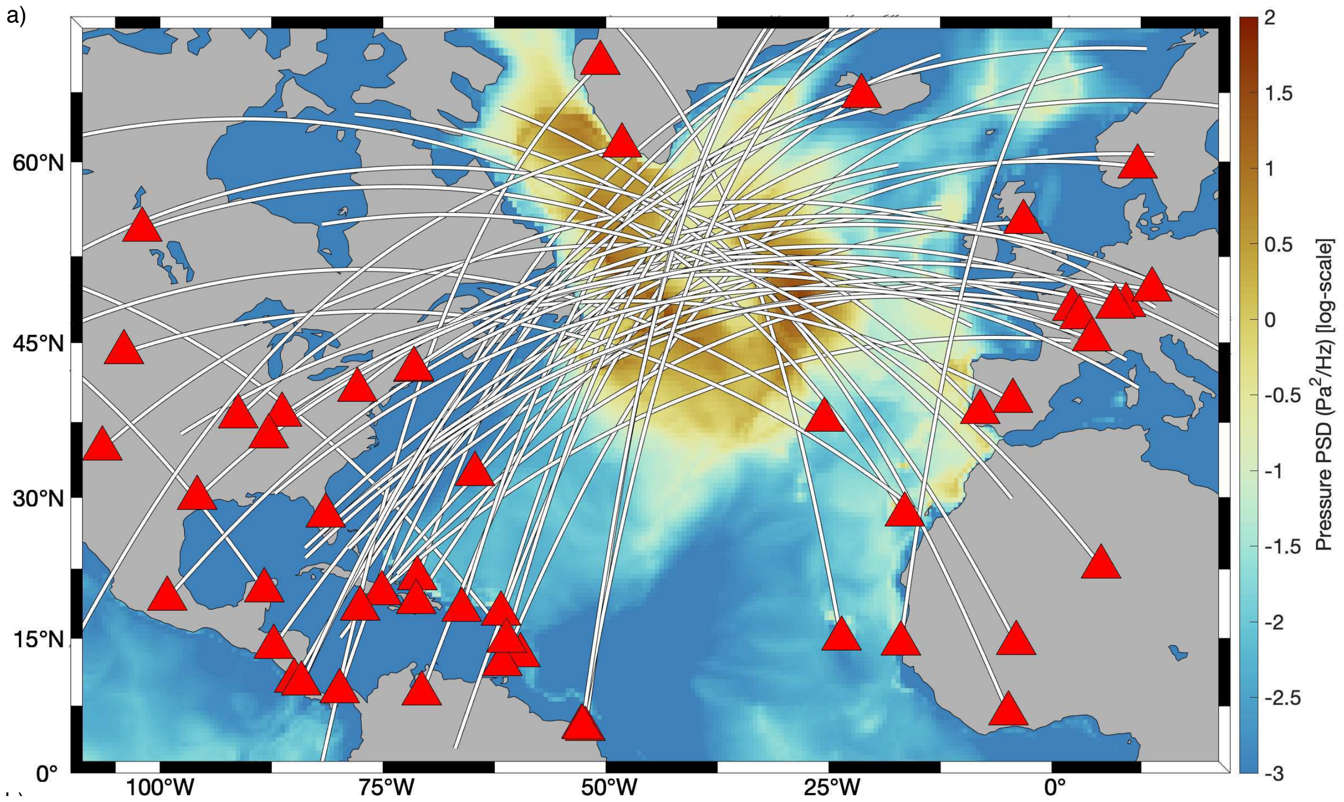

Figure 1: *Great-circle paths along the main direction of arrival for stations around the North Atlantic Ocean, as computed in 3-D Earth model S40RTS in the presence of bathymetry. The background color represents the median pressure power spectral density of the oceanic sources. Stations from the Global Seismographic Network were vital to conducting this study.* `http://doi.org/10.1073/pnas.2013806117` *and* `http://doi.org/10.1093/gji/ggab095`

The mantle transition zone beneath eastern North America

Alexander L. Burky, Jessica C.E. Irving & Frederik J. Simons

Princeton University | University of Bristol

The eastern continental margin of North America, despite being a passive margin at present, records a comprehensive tectonic history of both mountain building and rifting events. This record is punctuated by several igneous events, including those associated with the Great Meteor and Bermuda hotspots. To gain a better understanding of the state of the mantle beneath this region, we employ USArray data to image the mantle transition zone beneath eastern North America. We first calculate P-to-s receiver functions using an iterative time-domain deconvolution algorithm. These receiver functions are then automatically filtered by their quality, using a set of rigorous criteria, and subsequently summed using common conversion point stacking. Cross sections through these stacks show remarkable features such as a thinned transition zone beneath the independently observed northern Appalachian and central Appalachian low-wavespeed anomalies, as well as a thickened transition zone beneath western Tennessee associated with the Laramide slab stagnating at depth. A technical analysis of the effects of using various seismic velocity models for the moveout correction of our receiver functions reveals that the thickness of the mantle transition zone under eastern North America is a robust measurement, while the resolved depths of the 410 and 660 km discontinuities are model dependent.

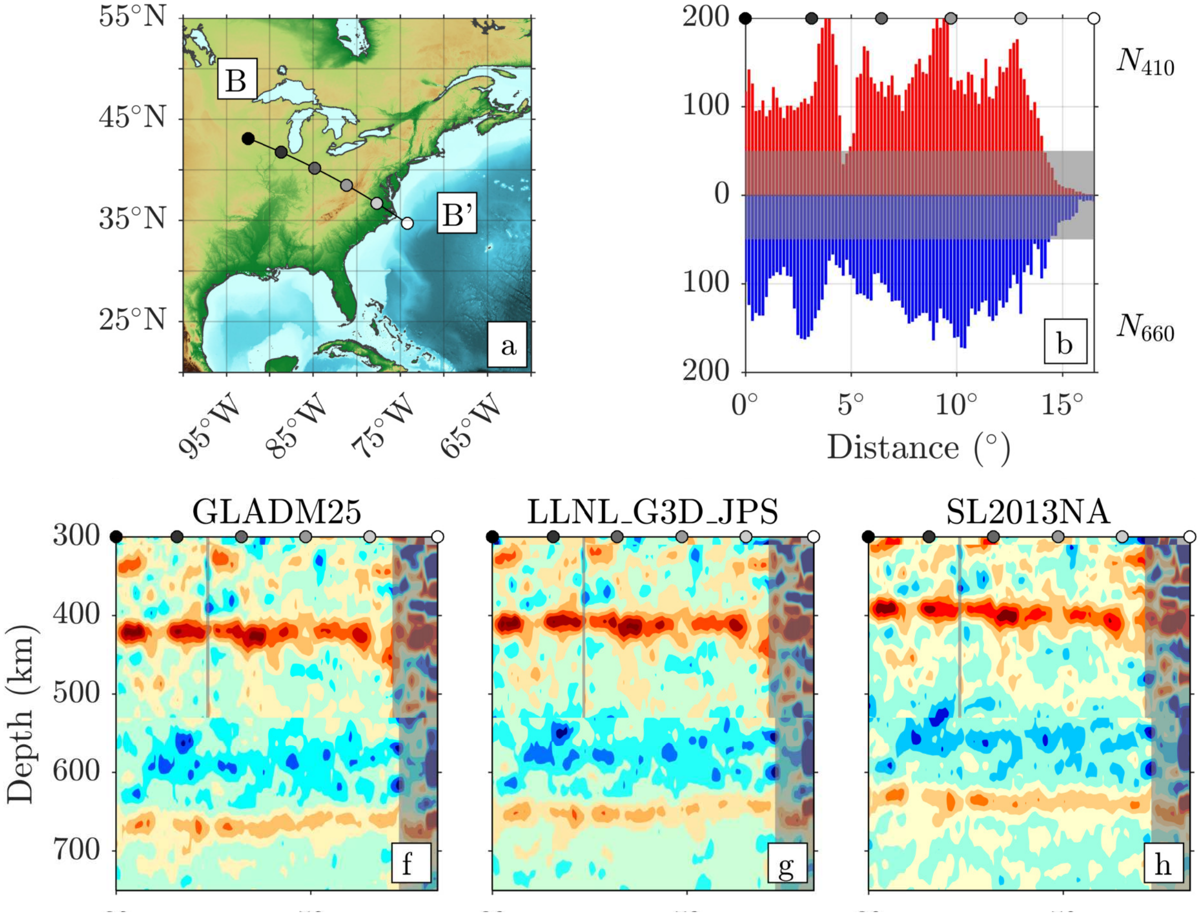

Figure 1: *Mantle transition zone (MTZ) structure in the region of the Central Appalachian Anomaly. Note the considerable amount of topography on the 410 discontinuity, and the strong thinning of the MTZ at the SE end of the cross section. Also note the data sparsity and poor resolution at the southeasternmost end of this cross section. The negative-polarity signals around 600 km depth are most likely artifacts from filtering and the presence of PcP.*

Waveform modeling of seismic records from MERMAID (the ultimate emerging hardware and software)

Sirawich Pipatprathanporn & Frederik J. Simons

Princeton University

Thousands of seismograms have been reported by MERMAID (Mobile Earthquake Recording in Marine Areas by Independent Divers), an oceanic float that detects earthquakes in remote regions. MERMAID seismograms have been used for travel-time tomography, but modeling the entire waveform has remained elusive. What prevented the application of Full-Waveform Inversion (FWI) to MERMAID seismograms is that simulating wave propagation in a 3-D global domain with an ocean in which acoustic waves propagate is too computationally expensive at the frequencies 0.1–10 Hz, where MERMAIDsinstrument response is flat. Our solution is to split the simulation into a part that models the response of the solid Earth from the earthquake source to the ocean bottom, and another that models the wave propagation within the ocean layer. For the first part, we use Instaseis, with precomputed elastic Green's functions, to obtain displacement seismograms within a 1-D Earth model. For the second part, we first use SPECFEM-2D to solve the elastic and acoustic wave equations, taking into account bathymetry and pressure wave propagation within the water column. The simulations return time series of vertical displacement at the ocean bottom due to incoming plane waves, and acoustic pressure at the MERMAID depth. We de-convolve them to obtain a catalog of response functions between the displacement at the conversion point of plane waves from distant earthquake sources and the sound pressure, for a variety of environments and ray parameters. For any particular earthquake-receiver pair, we then convolve the vertical displacement from Instaseis with the appropriate response function to model hydroacoustic pressure waveforms observed by MERMAID. In this way can successfully model MERMAID records within the first few seconds following the first P-wave arrival, within a frequency band determined dynamically. The correlation between synthetics and observations in our vast collection is as high as 0.98, with a median of 0.72, and very coherent across the array, allowing for the determination of cross-correlation travel times and opening up MERMAID seismograms to conduct full-waveform tomography of Earth's mantle.

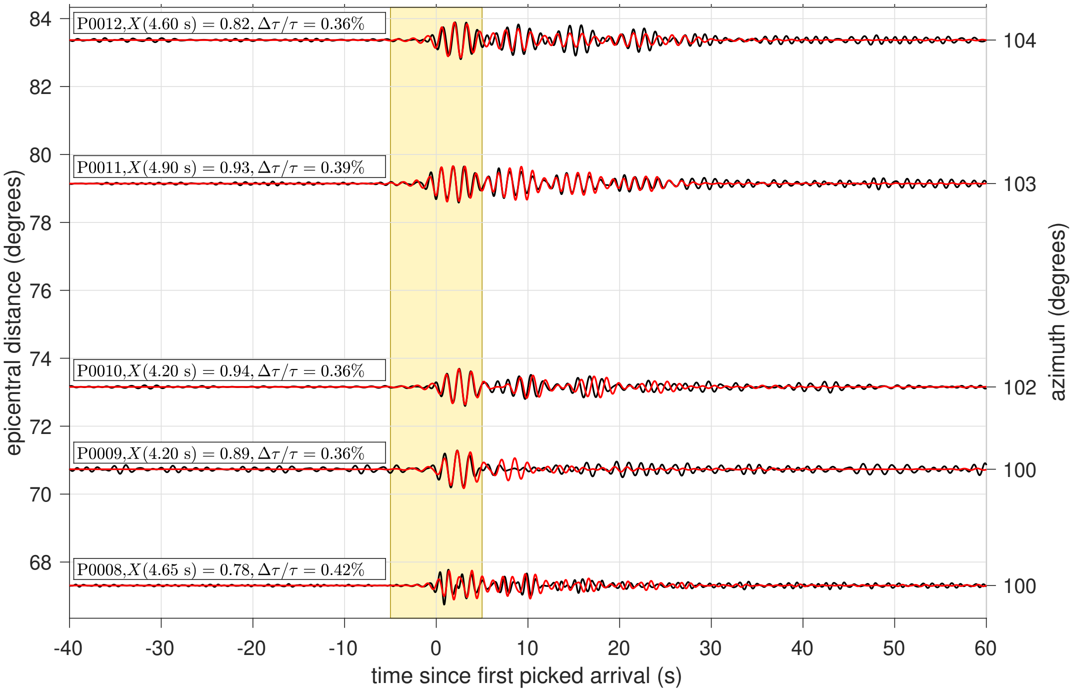

Figure 1: Waveform modeling of MERMAID records of CMT event C201808171535A, magnitude 6.50, depth 529.00 km. Indicated are MERMAID name and number, cross correlation argmax and value, and the relative travel-time anomaly (in per cent). MERMAID was designed capture high-frequency P-wave travel times, but its lower-frequency waveforms can be modeled with great accuracy and precision, allowing for detailed analysis.